Multi-cavity optoelectronic oscillators using multicore fibers

Sergi García and Ivana Gasulla[1,*]

[1]*ITEAM Research Institute, Universitat Politécnica de Valencia, Camino de Vera s/n, 46022 Valencia, Spain*
**ivgames@iteam.upv.es*

Abstract: We propose the use of both homogeneous and heterogeneous multicore fibers to implement multi-cavity optoelectronic oscillators. We present design equations and examples that show the potential for unique performance in terms of spectral selectivity, tunability and high-frequency operation.

OCIS codes: (060.2360) Fiber optics links and subsystems; (060.5625) Radio frequency photonics; (130.0250) Optoelectronics; (350.4010) Microwaves.

References and links

1. Technology focus on Microwave photonics, Nat. Photonics **5**, 723-736 (2011).
2. J. Capmany, J. Mora, I. Gasulla, J. Sancho, J. Lloret, and S. Sales, "Microwave photonic signal processing," J. Lightwave Technol. **31**, 571-586 (2013).
3. A. Seeds, "Microwave photonics," IEEE Trans. Microwave Theory Tech. **50**, 877-887 (2002).
4. I. Gasulla and J. Capmany, "Microwave photonics applications of multicore fibers," Photonics J. **4**, 877-888 (2012).
5. D.J. Richardson, J.M. Fini, and L.E. Nelson, "Space division multiplexing in optical fibers," Nat. Photonics **7**, 354-362 (2013).
6. M. Koshiba, K. Saitoh, and Y. Kokubun, "Heterogeneous multi-core fibers: Proposal and design principle," IEICE Electron. Exp. **6**, 98-103 (2009).
7. A. Sano et al., "409-Tb/s + 409-Tb/s crosstalk suppressed bidirectional MCF transmission over 450 km using propagation-direction interleaving," Opt. Express **21**, 16777-16783 (2013).
8. D. Barrera, I. Gasulla and S. Sales, "Multipoint two-dimensional curvature optical fiber sensor based on a non-twisted homogeneous four-core fiber," J. Lightwave Technol. (in press).
9. X.S. Yao and L. Maleki, "Converting light into spectrally pure microwave oscillation," Opt. Lett. **21**, 483-485 (1996).
10. X.S. Yao and L. Maleki, "Optoelectronic microwave oscillator," J. Opt. Soc. Am. B **8**, 1725-1735 (1996).
11. X.S. Yao and L. Maleki, "Opto-electronic oscillator for photonic systems," IEEE J. Quantum Electron. **32**, 807-814 (1996).
12. A.B. Matsko, L. Maleki, A.A. Savchenkov, and V.S. Ilchenko, "Whispering gallery mode based optoelectronic microwave oscillator," J. Modern Opt. **50**, 2523-2542 (2003).
13. K. Volyanskiy, P. Salzenstein, H. Tavernier, M. Pogurmirskiy, Y. K. Chembo, and L. Larger, "Compact optoelectronic microwave oscillators using ultra-high Q whispering gallery mode disk-resonators and phase modulation," Opt. Express **18**, 22358-22363 (2010).
14. D. Eliyahu, W. Liang, E. Dale, A.A. Savchenkov, V. S Ichenko, A. B. Matsko, D. Seidel, and L. Maleki, "Resonant widely tunable opto-electronic oscillator," IEEE Photon. Tech. Lett. **15**, 1535-1538 (2013).
15. K. Saleh, R. Henriet, S. Diallo, G. Lin, R. Martinenghi, I. V. Balakireva, P. Salzenstein, A. Coillet, and Y. K. Chembo, "Phase noise performance comparison between optoelectronic oscillators based on optical delay lines and whispering gallery mode resonators," Opt. Express **22**, 32158-32173 (2014).
16. M. Aspelmeyer, T.J. Kippenberg and F. Marquardt, "Cavity optomechanics," Rev. Mod. Phys. **86**, 1391-1452 (2014).
17. X.S. Yao and L. Maleki, "Dual microwave and optical oscillator," Opt. Lett. **22**, 1867-1869, (1997).
18. X.S. Yao, L. Davis and L. Maleki, "Coupled optoelectronic oscillators for generating both RF signals and optical pulses," J. Lightwave Technol. **18**, 73-78 (2000).
19. A.B. Matsko, D. Eliyahu, P. Koonath, D. Seide and L. Maleki, "Theory of coupled optoelectronic microwave oscillator I: expectation values," J. Opt. Soc. Am. B **26**, 1023-1031 (2009).

20. A.B. Matsko, D. Eliyahu and L. Maleki, "Theory of coupled optoelectronic microwave oscillator II: phase noise," J. Opt. Soc. Am. B **30**, 3316-3323 (2013).
21. X.S. Yao and L. Maleki, "Multiloop optoelectronic oscillator," IEEE J. Quantum Electron. **36**, 79-84 (2000).
22. T. Bánky, B. Horváth and T. Berceli, "Optimum configuration of multiloop optoelectronic oscillators," J. Opt. Soc. Am. B **23**, 1371-1380 (2006).
23. J. Capmany and M.A. Muriel, "A new transfer matrix formalism for the analysis of fiber ring resonators: compound coupled structures for FDMA demultiplexing," J. Lightwave Technol. **8,** 1904-1919 (1990).
24. M. Koshiba, "Design aspects of multicore optical fibers for high-capacity long-haul transmission," *in Proceedings of IEEE 2014 Int. Topical Meeting on Microwave Photonics* (IEEE, 2014), pp. 318-323.
25. S. Garcia and I. Gasulla, "Design of heterogeneous multicore fibers as sampled true time delay lines," Opt. Lett. (in press).
26. D.B. Leeson, "A simple model of feedback oscillation noise spectrum," IEEE Proc. **54**, 329-330 (1966).
27. S.G. Leon-Saval, A. Argyros, and J. Bland-Hawthorn, "Photonic lanterns: a study of light propagation in multimode to single-mode converters," Opt. Express **18**, 8430-8439 (2010).

1. Introduction

Microwave photonics (MWP) is an interdisciplinary area that pursues the generation, processing and distribution of microwave and millimeter-wave signals by photonic means, [1-3]. The widespread adoption of MWP is limited, on the one hand, by the bulky and heavy nature of the current signal generation and processing solutions, and on the other hand, by the lack of compact and efficient parallel architectures in the deployed distribution networks. To solve these limitations and reduce the associated cost impact, we have proposed for the first time the extension of the concept of Space-Division multiplexing (SDM), currently restricted to high-capacity digital communications, to the areas of analog photonics and radio-over fiber, [4]. More specifically, we have proposed to exploit the inherent parallelism of multicore fibers (MCFs) to implement a sampled discrete True time delay line (TTDL) for radiofrequency (RF) signals featuring unique properties beyond the current state of the art.

The exploitation of the last available degree of freedom for optical multiplexing -space- has been recently researched as a solution to the upcoming capacity bottleneck in Digital Communications, [5-7]. The future optical network can benefit from MCFs by establishing independent light paths in a single optical fiber through a set of physically distinct singlemode cores that are confined inside a single cladding, [5]. Most of the research activity on SDM has employed the so-called homogeneous MCFs, where all the cores are identical and thus share the same propagation characteristics. Cross coupling between the cores and the resulting crosstalk can be reduced by keeping the cores well-spaced and further mitigated by introducing trench-assisted configurations around each core. Heterogeneous MCFs, where the cores have different material composition or refractive index profile, have also been proposed to drastically decrease the inter-core crosstalk [6]. Previous work on digital SDM transport networks reported minimum crosstalk levels around -50 dB, e.g. bidirectional 409-Tb/s transmission over a 450-km link [7], a figure well below the -25 dB considered as the maximum crosstalk enough to avoid significant transmission penalties for most signal modulation formats.

The MCF structure also provides an ideal environment for the parallel propagation of signals subject to identical mechanical and environmental conditions, and thus can be considered for a wider range of application fields including sensors [8] and microwave photonics [4]. In this last field a particularly attractive application is the implementation of optoelectronic oscillators (OEOs). Initially proposed by Yao and Maleki [9-11], single cavity OEOs can provide ultra-stable, tunable and extremely low-linewidth RF frequency generation in a broad frequency range. High spectral-purity signal generation in single cavity OEOs requires a long fiber loop, what results in the generation of a considerable number of oscillation modes and the need to incorporate very selective RF filters in the electronic part of the system. To combat this limitation, several solutions have been proposed to refine and improve the performance of OEOs, including the incorporation of a highly selective whispering gallery

optical filter in the optical segment of the oscillator [12] that can lead to extremely compact [13], broadly tunable [14] and low phase noise [15] devices with the possibility of exploiting as well opto-mechanical effects [16]. Coupled optoelectronic oscillators (COEOs), which simultaneously produce spectrally pure microwave signals as in a OEO and short optical pulses as in a mode locked laser, have also been proposed and actively researched during the last years [17-20]. Finally, multi-cavity or multiloop OEOs have been proposed [21], where a long cavity provides the required spectral purity and a short fiber cavity provides the required spectral separation between adjacent oscillating modes, what alleviates the narrowband requirement for the internal RF filter. Furthermore, these structures can be generalized to an arbitrary number of loops and its design optimized for cavity lengths that are multiple of a given reference value [22].

In this paper we propose the use of MCFs for the implementation of multi-cavity OEOs. MCF provides an ideal medium for the implementation of multiple parallel cavities, all of which will be subject to practically identical mechanical and environmental conditions. In section 2 we extend the theory developed in [21,22] for the case of two cavity OEOs to a general number N of cavities providing the equations describing the oscillation spectrum, amplitude and phase oscillation conditions, and phase noise spectrum. We describe in section 3 the proposed configurations based on homogeneous MCFs, where we consider two separate cases: a first one corresponding to two (short and long) unbalanced cavities, as reported in [21] and optimized in [22]; and a second one related to N almost equal length cavities working under the vernier configuration [23]. In section 4 we analyze a configuration based on a heterogeneous MCF, showing as well that this particular scheme allows tunability of the oscillation frequency by operating the OEO with a tunable laser. In practical terms, the required MCFs feature lengths ranging from a few meters to < 10 km. For these values the expected impact of intercore crosstalk is below < -70 dB [24], which will have a negligible impact on the independent cavity operation.

2. Multi-cavity OEO model

2.1 Signal

Figure 1 shows the general layout of the multi-cavity OEO considered in this paper. A common optical source, modulator, RF amplifier, photodetector and RF filter are shared by the different cavities (here labeled as $k = 1, 2,... N$). Each cavity is implemented in the optical domain using different cores of a single multicore fiber and features a different round-trip complex-valued gain g_k, given by:

$$\begin{aligned} |g_k| &= G_k \left| H_k(\omega) \right|, \\ \phi_k &= \arg\left[H_k(\omega) \right]. \end{aligned} \tag{1}$$

where G_k represents the voltage gain coefficient and $\tilde{H}_k(\omega) = |H_k(\omega)| \exp(\mathrm{j}\phi_k)$ the unitless complex filter function that accounts for the combined effect of all frequency dependent components in the cavity. Our proposal can be considered an extension of earlier reported systems for three reasons. In first place, as we will see, it allows not only for the implementation of multiple cavity OEOs where cavity lengths are a multiple of a given reference value, as proposed in [21 22], but also of multiple cavity OEOs where cavity lengths are slightly different exploiting the Vernier effect. In second place, the use of a single multicore fiber structure to host all the cavities provides an integrated hosting medium for enhancing their relative stability against environmental fluctuations. In third place, if properly designed heterogeneous MCFs are employed [25], then tunable multiploop OEOs can be potentially implemented.

Following a similar procedure as Yao and Maleki [21], the recursive relationship for the complex amplitude of the circulating field after the r^{-th} round-trip can be expressed as:

$$\tilde{V}_r(\omega) = \tilde{V}_{r-1}(\omega)\left[\sum_{k=1}^{N}|g_k|e^{j(\omega\tau_k+\phi_k)}\right]. \tag{2}$$

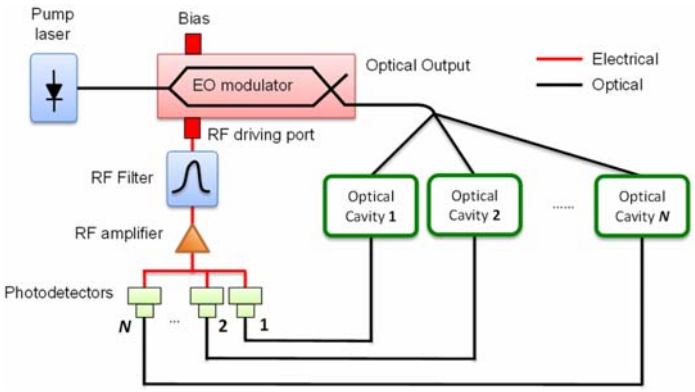

Fig. 1. Layout of a multi-cavity optoelectronic oscillator.

Hence, if the oscillation starting voltage is given by $G_a\tilde{V}_{in}(\omega)$ where G_a is the RF amplifier voltage gain, then the application of Eq. (2) yields:

$$\tilde{V}_{out}(\omega) = \sum_{r=0}^{\infty}\tilde{V}_r(\omega) = \frac{G_a\tilde{V}_{in}(\omega)}{1-\sum_{k=1}^{N}|g_k|e^{j(\omega\tau_k+\phi_k)}} \tag{3}$$

and the corresponding RF power:

$$P(\omega) = \frac{\left|\tilde{V}_{out}(\omega)\right|^2}{2R} = \frac{G_a^2\left|\tilde{V}_{in}(\omega)\right|^2/2R}{1+\sum_{k=1}^{N}|g_k|^2+2\sum_{\substack{k=1\\l>k}}^{N}|g_k||g_l|\cos\left[\Phi_k(\omega)-\Phi_l(\omega)\right]-2\sum_{k=1}^{N}|g_k|\cos\left[\Phi_k(\omega)\right]} \tag{4}$$

where R represents the load impedance of the RF amplifier and:

$$\Phi_k(\omega) = \omega\tau_k + \phi_k. \tag{5}$$

For oscillations to start collectively in all the cavities at an angular frequency ω_o we need:

$$\begin{aligned}&\Phi_k(\omega_o) = 2m_k\pi;\\ &\Phi_k(\omega_o)-\Phi_l(\omega_o) = 2(m_k-m_l)\pi; \qquad m_k, m_l \in Z.\end{aligned} \tag{6}$$

Under these conditions then:

$$P(\omega_o) = \frac{G_a^2\left|\tilde{V}_{in}(\omega_o)\right|/2R}{1+\sum_{k=1}^{N}|g_k|^2+2\sum_{\substack{k=1\\l>k}}^{N}|g_k||g_l|-\sum_{k=1}^{N}|g_k|}. \tag{7}$$

For oscillations to start from noise the denominator in Eq. (7) must vanish:

$$1+\sum_{k=1}^{N}\left|g_k\right|^2+2\sum_{\substack{k=1\\l>k}}^{N}\left|g_k\right|\left|g_l\right|-\sum_{k=1}^{N}\left|g_k\right|=0. \tag{8}$$

A simple case is when the gain coefficients have equal moduli in all cavities $|g_k| = g, \ \forall\ k$ in which case, Eq. (8) leads to:

$$|g| = 1/N \tag{9}$$

2.2 Noise

The noise model for the multi-cavity OEO follows from the double-cavity case developed by Yao and Maleki [9], where the starting oscillations build up from the RF noise power at the photodetector output, hence:

$$\rho_N(\omega)\Delta f=\frac{\left|\tilde{V}_{in}(\omega)\right|^2}{2R}, \tag{10}$$

where $\rho_N(\omega)$ is the power spectral density of the input noise and Δf its bandwidth. $\rho_N(\omega)$ given by Eq. (30) in [10] takes into account all the technical noise sources in the OEO, including thermal, shot, relative intensity noise and, when applicable, amplified spontaneous emission noise. It is usually represented by a value in the range of -180 to -160 dB/Hz [10,22]. Substituting Eq. (10) into Eq. (4) and taking Eq. (5) and Eq. (6) into consideration, we find the following expression for the power spectral density of the mode oscillating at ω_o:

$$S_{RF}(f')\equiv\frac{P(f')}{\Delta f P_{osc}}=\frac{G_a^2\rho_N^2/P_{osc}}{1+\sum_{k=1}^{N}\left|g_k\right|^2+2\sum_{\substack{k=1\\l>k}}^{N}\left|g_k\right|\left|g_l\right|\cos\left[2\pi f'(\tau_k-\tau_l)\right]-2\sum_{k=1}^{N}\left|g_k\right|\cos\left[2\pi f'\tau_k\right]} \tag{11}$$

being $f'=\dfrac{\omega-\omega_o}{2\pi}$ the offset frequency from the RF carrier,

where P_{osc} represents the RF oscillation power. Alternatively, one can use the method developed by Leeson [26] to express the phase noise in terms of the loaded cavity quality factor.

3. Multi-cavity OEOs using homogeneous multicore fibers

Homogeneous multicore fibers are structures in which a single cladding surrounds N cores with equal propagation (singlemode or few-mode operation) and transmission characteristics (losses, chromatic dispersion). Typical values of N for reported devices are N = 7, 10, 12 and 19. Loss coefficients are in the range of 0.18 and 0.29 dB/km @1550 nm [24]. A key parameter is also the crosstalk between cores, which ranges in between -72 and -22 dB/100 km. The lowest values are obtained using special trench designs for the refractive index profiles of the cores. Taking into consideration, as we will see, that MCF lengths required for OEOs range in between a few meters and a few km, it is expected that intercore crosstalk will have a negligible impact. Furthermore, since same cladding will host all the cores, and therefore all the cavities, it is reasonable to expect that all these cavities will be subject to identical mechanical and environmental conditions.

The identical multiple cores of a homogeneous MCF can be employed to implement both double- and multiple cavity OEOs. We now treat each case separately.

3.1 Double unbalanced cavity OEOs

The left part of Fig. 2 shows the layout of a double-cavity OEO [11] based on an N-core homogeneous MCF. Here k_1 ($k_1 < N/2$) cores are linked to form the first (short) cavity while the remaining N-k_1 cores form the second (long) cavity. If the core lengths are all equal to L and the group delay per unit of length is given by τ_{go}, then each core provides a group delay given by $\tau = \tau_{go} L$.

The oscillation frequency must verify:

$$f_o = \frac{m}{k_1 \tau_{go} L} \qquad m = 1, 2, \ldots . ;$$
$$f_o = \frac{n}{(N - k_1)\tau_{go} L} \qquad n = 1, 2, \ldots . \quad . \tag{12}$$

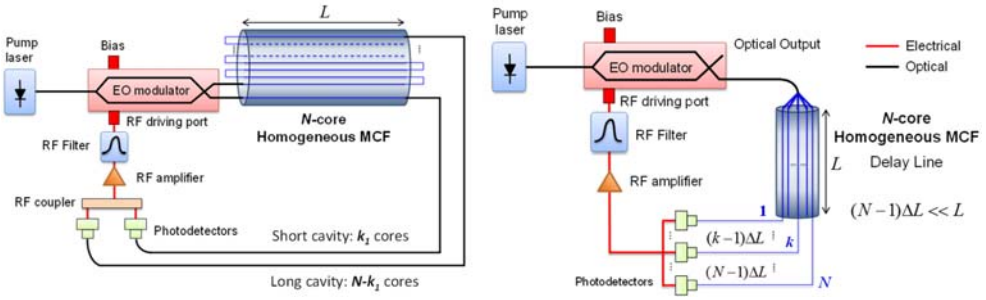

Fig. 2. (Left) Double unbalanced cavity OEO using an N-core homogeneous MCF. (Right) Multiple cavity OEO with almost equal length (vernier OEO).

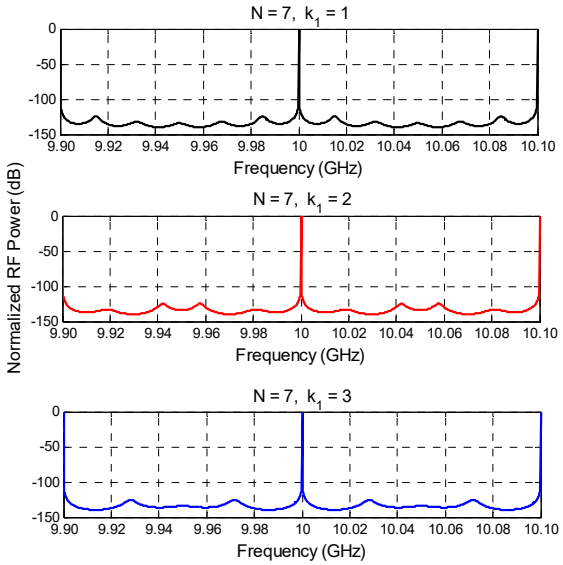

Fig. 3. Oscillation spectra for a double unbalanced cavity OEO using a 2-meter 7-core homogeneous MCF as a delay cavity. (Upper) Configuration with a short cavity of 2 m and a long cavity of 12 m. (Middle) Configuration with a short cavity of 4 m and along cavity of 10 m. (Lower) Configuration with a short cavity of 6 m and a long cavity of 8 m.

The first expression in Eq. (12) is employed to determine the required value of L, taking as a starting point the knowledge of f_o, N, k_1, τ_{go} and a set value for m. Once the value of L is set, the value of n is obtained from the second expression in Eq. (12). For example, for an oscillation frequency of f_o = 10 GHz, and a typical seven core MCF (N = 7), if k_1 = 1 and τ_{go} = 5 ns/m,

setting m = 1000 yields L = 2 m and n = 6000, leading to a short cavity of 2 m and a long cavity of 12 m. If k_1 = 2 and L is kept fixed to 2 m, then m = 2000 and n = 5000 leading to a short cavity of 4 m and a long cavity of 10 m. If k_1 = 3 then m = 3000 and n = 4000 leading to a short cavity of 6 m and a long cavity of 8 m. Figure 3 shows the oscillation spectra for these three cases, where an RF filter centered at 10 GHz and with maximum bandwidth of 100 MHz is enough for single-mode oscillation.

In all the cases the spectrum periodicity is set by the short cavity while the resonance linewidth is imposed by the longer cavity. The computed results for the OEO phase noise spectra are shown in Fig. 4. For the computation we have employed standard noise (ρ_n = -180 dBm/Hz), RF gain (G_a = 10) and oscillation power (P_{osc} = 16 dBm) values. The results show almost identical phase behavior in terms of linewidth, as the change in the longer cavity length (4 m) has an almost negligible effect in the resonance quality factor. The high level of phase noise close to the carrier can be explained by the fact that the longest cavity length ranges from 8 to 12 m. Since the phase noise is dominated by the spectral width of the longest cavity resonance [21], a high level is expected.

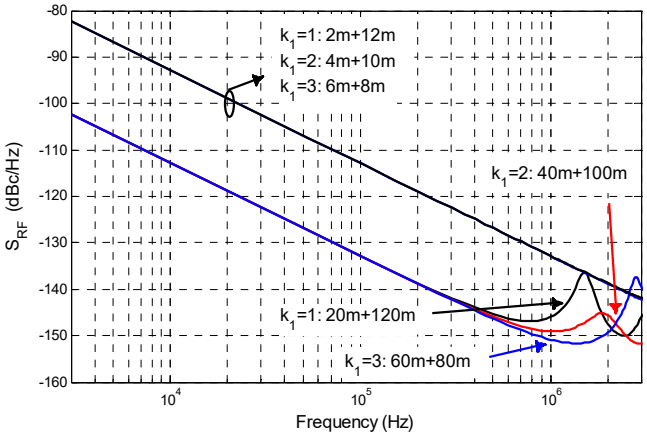

Fig. 4. (Upper traces) Phase noise spectra computed for the three cases of Fig. 3. (Lower traces) Phase noise spectra computed for the same three cases when L = 20 m. Standard noise (ρ_n = -180 dBm/Hz), RF gain (G_a = 10) and oscillation power (P_{osc} = 16 dBm) values have been employed.

It is possible to improve the phase noise characteristic by extending the basic cavity length. In the former example setting m = 10000 yields L = 20 m and n = 60000, leading to a short cavity of 20 m and a long cavity of 120 m. If k_1 = 2 and L is kept fixed to 20 m, then m = 20000 and n = 50000 leading to a short cavity of 40 m and a long cavity of 100 m. If k_1 = 3 then m = 30000 and n = 40000 leading to a short cavity of 60 m and a long cavity of 80 m. Oscillation at 10 GHz requires however an RF filter with a 10 MHz bandwidth. Fig. 4 shows for comparison the results for the longer cavity design where a 20 dB reduction is observed.

Of course, as reported in [22], these OEOs can be optimized provided a given procedure is followed that entails the adjustment of the phase response of the open cavity transfer function, so there is only one frequency that fulfills the round-trip constructive phase condition. To do this, the cavity gain coefficients must be carefully tailored to follow a different law than that given by Eq. (9). We present here an optimized design for a 3-cavity OEO based on a 19-core MCF following the guidelines of [22], which can be considered for assembly in a laboratory experiment. For an oscillation frequency of 10 GHz, we choose a basic cavity delay of τ = 26.3 ns and three cavities providing τ, 6τ and 11τ, which amount to fiber lengths given by 5.26, 31.56 and 57.86 m, respectively. These can be implemented using 18 cores of a 5.26-m long 19-core homogeneous MCF. The first cavity is provided by a single core, the second by folding back the propagation through 6 cores and the longest one by folding back the propagation through

11 cores. The optimized coefficients for the phase transmission function of the OEO are given by $g_1 = 0.48$ (for the τ cavity), $g_2 = 0.22$ (for the 6τ cavity) and $g_3 = 0.3$ (for the 11τ cavity). The right upper part of Fig. 5 shows the open loop phase transmission of the three-loop optimized cavity. The left upper part shows a detail of the oscillation spectra around 10 GHz and the lower part details the phase noise computed again for standard noise (ρ_n = -160 dBm/Hz), RF gain (G_a = 10) and oscillation power (P_{osc} = 16 dBm) values. The phase noise characteristic is very similar to that reported in [22] for a 3-cavity OEO and, in consequence, one should expect a very similar performance when assembling this structure in an experimental setup.

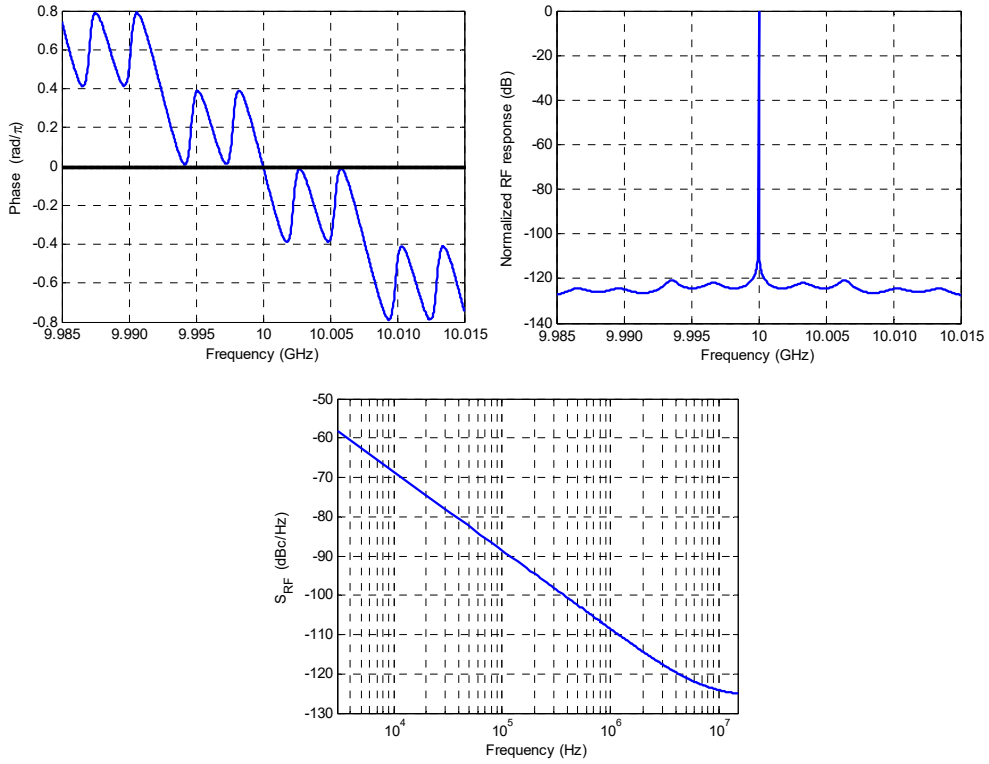

Fig. 5. Open loop phase transmission (upper left), oscillation spectra (upper right), and phase noise (lower) for an optimized multi-cavity OEO based on a 5.26 m homogeneous 19-core MCF. Standard noise (ρ_n = -160 dBm/Hz), RF gain (G_a = 10) and oscillation power (P_{osc} = 16 dBm) values have been employed.

3.2 Multi-cavity vernier OEOs

The right part of Fig. 3 shows the layout for a multiple cavity OEO where the different cores of the MCF are employed to build cavities with slightly different physical length. Here the homogeneous MCF with core length L is coupled to an output photonic lantern [27] with different (but evenly spaced by ΔL) physical lengths in its output ports. This photonic lantern features in consequence incremental delays between adjacent ports given by $\Delta\tau = \tau_{go}\,\Delta L$. In this case Eq. (5) results:

$$\Phi_k(\omega) = \omega\tau_{go}L + (k-1)\omega\tau_{go}\Delta L + \phi_k \quad \text{for } k = 1, 2, \ldots N. \tag{13}$$

Assuming $\phi_k = 0\ \forall\ k$, the oscillation frequency must verify:

$$f_o = \frac{m}{\tau_{go} L}, \tag{14}$$

which is employed to determine the required value of L taking as a starting point the knowledge of f_o, τ_{go} and a set value for m. For the rest of the cavities, in order to have vernier effect [13] operation and constructive interference at f_o, we require:

$$2\pi f_o \Delta\tau = 2\pi \;\Rightarrow\; f_o = \frac{1}{\tau_{go}\Delta L}. \tag{15}$$

From Eq. (14) and Eq. (15) we have $L/\Delta L = m$. Hence, although the free spectral range of each cavity is approximately $1/\tau$, the free spectral range value of the coupled-cavity configuration is $1/\Delta\tau = m/\tau$ due to the vernier effect. For example, for an oscillation frequency f_o = 10 GHz and a MCF featuring τ_{go} = 5 ns/m setting m = 1000 yields L = 20 m and ΔL = 2 cm, which is an incremental value that can be easily achieved in a compact photonic lantern device closing the MCF. Figure 6 shows the oscillation spectra for this example computed from Eq. (4) when a 7-core fiber is considered and the number of parallel cavities ranges from 2 to 7.

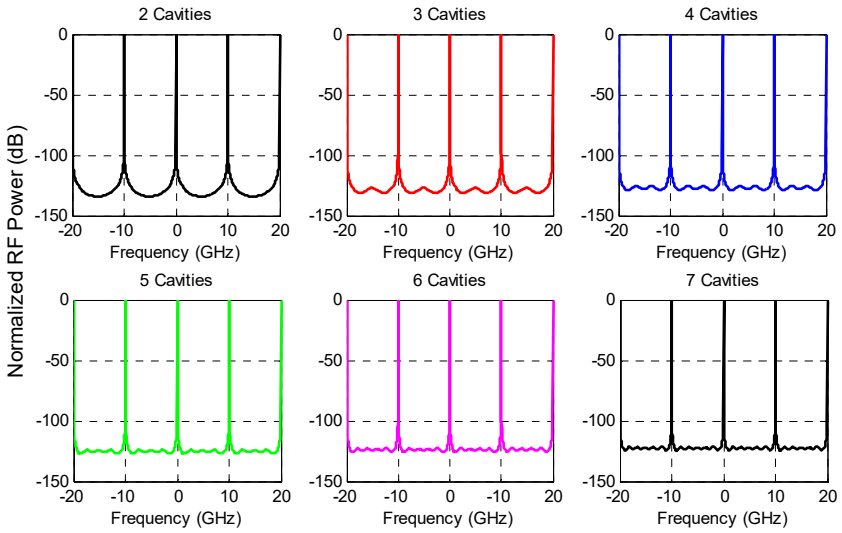

Fig. 6. Oscillation spectra for a multi-cavity vernier OEO using a 20-meter 7-core homogeneous fiber.

It is remarkable that in all the cases the overall coupled cavity free spectral range is 10 GHz, despite the fact that the free spectral range values for the individual cavities are around 10 MHz. In consequence, mode selection does not require a selective RF filter since a bandwidth of 1 GHz is more than enough to select the 10-GHz oscillation line. Adding more cavities apparently results in a reduction in the oscillation linewidth. An interesting feature of this configuration is that the spurious modes generated in this OEO configuration are further rejected by increasing the number of the involved cavities. As in the former case, we also computed the phase noise spectra for standard noise (ρ_n = -180 dBm/Hz), RF gain (G_a = 10) and oscillation power (P_{osc} = 16 dBm) values. The results are almost independent from the number of cavities as these are very similar in length. For instance, when two cavities are considered the longest one is 20.02 m, while for the case of seven cavities, the longest one is 20.12 m. Under these conditions and bearing in mind that it is the longest cavity that dictates the noise linewidth, the differences can be considered negligible.

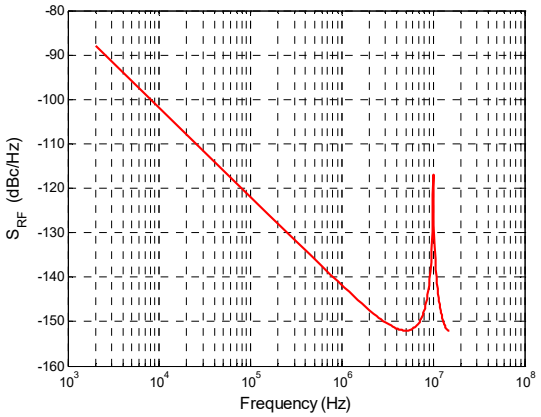

Fig. 7. Phase noise spectra computed for a multi-cavity vernier OEO using a homogeneous MCF for standard noise (ρ_n = -180 dBm/Hz), RF gain (G_a = 10) and oscillation power (P_{osc} = 16 dBm) values.

Figure 7 shows, as a representative example, the phase noise spectra for the case of 7 cavities. Where phase noise changes from -102 dBc/Hz at 10 kHz to -141 dBc/Hz at 1 MHz. Phase noise curves are all superimposed and no difference is appreciable. This can be explained as follows. For the case of two cavities, the longest cavity is 20.02 m featuring a free spectral range value of 10.334 MHz, while for the case of seven cavities, the longest cavity is 20.120 m with a corresponding free spectral range of 10.28 MHz. This results in a free spectral range relative difference of 0.5%. Since cavity lengths are so similar it is expected that loss difference due to propagation will be negligible and, therefore, the difference in the cavity finesse and in the resonance linewidth will also be around 0.5%.

4. Multi-cavity OEOs using heterogeneous multicore fibers

Heterogeneous MCFs have been proposed as a means to implement 2D (space and wavelength) tunable dispersive delay lines [4]. This property can be exploited to implement a tunable multi-cavity OEO. The basic proposed layout is shown in Fig. 8, where each core in the MCF has a different material and refractive index configuration to provide a different value of its dispersion parameter.

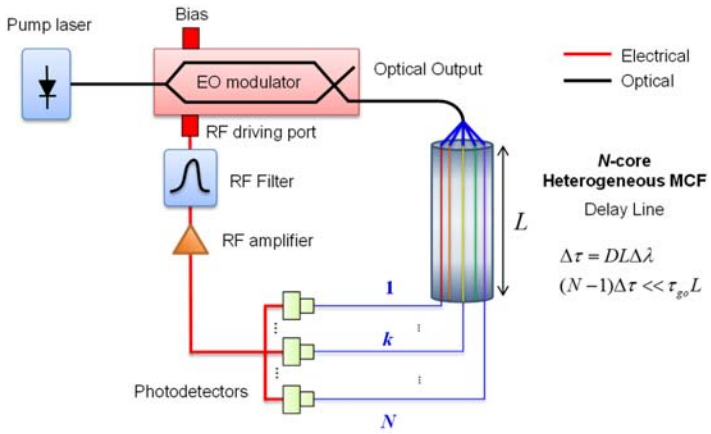

Fig. 8. Multi-cavity vernier OEO configuration using a heterogeneous MCF.

Of particular interest is the case where the dispersion parameter in each core is a multiple of a basic value D such that the delay provided by a core length L is given by [4]:

$$\tau_k = kDL\Delta\lambda + \tau_{go}L, \tag{16}$$

where τ_{go} is the group delay per unit of length at a given anchor wavelength λ_o and $\Delta\lambda = \lambda - \lambda_o$. In this case Eq. (5) transforms to:

$$\Phi_k(\omega) = \omega\tau_{go}L + k\omega DL\Delta\lambda + \phi_k \qquad \text{for } k = 1,2,...N. \tag{17}$$

Assuming $\phi_k = 0 \ \forall \ k$, the oscillation frequency must verify:

$$f_o = \frac{m}{\tau_{go}L + DL\Delta\lambda}. \tag{18}$$

For vernier operation at this frequency the incremental phase shift introduced by each cavity must provide constructive interference, hence:

$$f_o DL\Delta\lambda = 1. \tag{19}$$

Since D, τ_{go} and λ_o will normally be fixed, Eq. (18) and Eq. (19) provide the values of L and $\Delta\lambda$ once the value of m is fixed. Since the values of D are usually very small, the fulfillment of Eq. (19) will lead to multi-km cavity lengths for moderate $\Delta\lambda$ values leading to lower phase-noise characteristics as compared to homogeneous MCF OEO designs. For example, for an oscillation frequency f_o = 10 GHz and a MCF featuring τ_{go} = 5 ns/m and D = 1 ps/km.nm, Eq. (19) gives $L\Delta\lambda = 10^5$ n.nm. Therefore, one possible solution is given by L = 5 km and $\Delta\lambda$ = 20 nm. Figure 9 shows the oscillation spectra for this example computed from Eq. (4) when a heterogeneous 7-core fiber is considered and the number of parallel cavities ranges from 2 to 7.

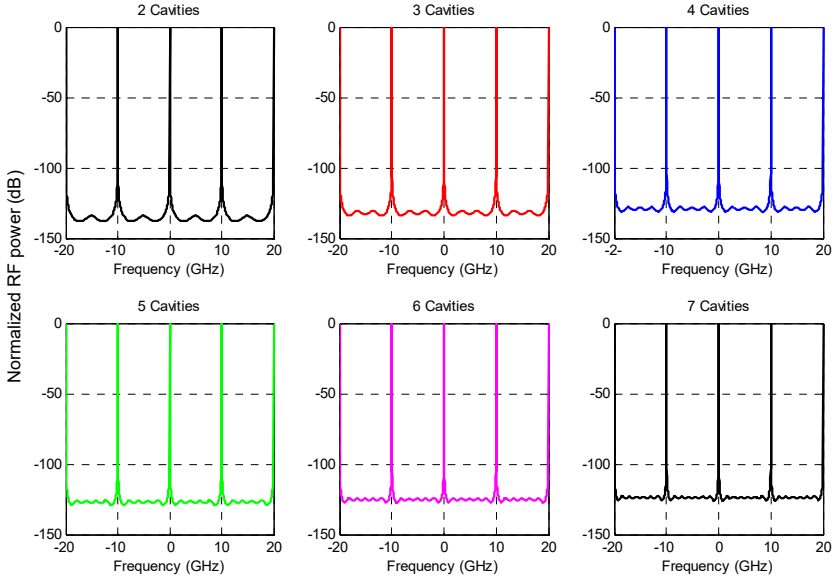

Fig. 9. Oscillation spectra for a multi-cavity vernier OEO using a 5-km, 7-core heterogeneous fiber.

In all the cases again the overall coupled cavity free spectral range is 10 GHz despite the fact that the free spectral range values for the individual cavities are around 40 kHz. In consequence, mode selection does not require a selective RF filter since a bandwidth of 1 GHz is more than enough to select the 10-GHz oscillation line. As in the homogeneous MCF case,

adding more cavities apparently results in a reduction in the oscillation linewidth. Again, as in the former case, we also computed the phase noise spectra for standard noise (ρ_n = -180 dBm/Hz), RF gain (G_a = 10) and oscillation power (P_{osc} = 16 dBm) values. The results are almost independent from the number of cavities as these provide almost the same delay. Figure 10 shows, as a representative example, the phase noise spectra for the case of 7 cavities, where phase noise changes from -110 dBc/Hz at 100 Hz to -150 dBc/Hz at 10 kHz.

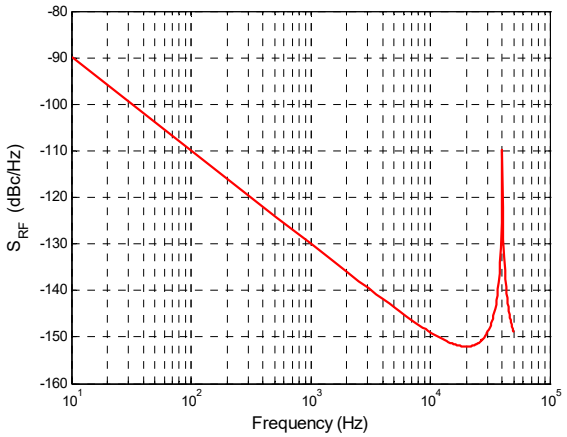

Fig. 10. Phase noise spectra computed for a multi-cavity vernier OEO using a heterogeneous MCF using standard noise (ρ_n = -180 dBm/Hz), RF gain (G_a = 10) and oscillation power (P_{osc} = 16 dBm) values.

A distinctive feature of this OEO, which follows from Eq. (19), is the possibility of tuning the oscillation frequency by changing $\Delta\lambda$, in other words, by using a tunable laser. For the example considered above, the specific relationship is f_o = 200 GHz / $\Delta\lambda$, where $\Delta\lambda$ is expressed in (nm). Figure 11 shows this relationship (left) and the oscillation frequencies (right) in between 10 and 20 GHz, computed from Eq. (4) for a set of selected values of $\Delta\lambda$.

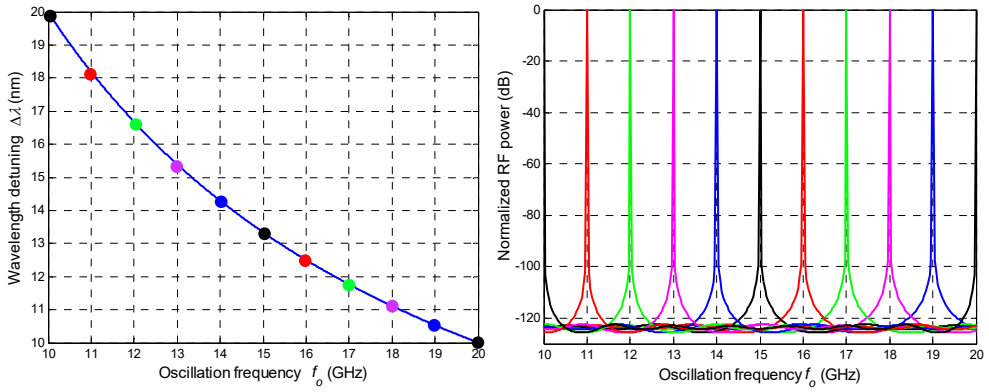

Fig. 11. Oscillation frequency vs wavelength detuning for a vernier multi-cavity OEO based on a 7-core heterogeneous fiber for τ_{go} = 5 ns/m, D = 1 ps/km.nm and L = 5 km.

5. Summary and conclusions

We have proposed the use of both homogeneous and heterogeneous multicore fibers for the implementation of multi-cavity optoelectronic oscillators. MCFs bring the advantage of hosting in a single compact structure the different cavities of the OEO. Design equations and examples

have been presented that show the potential of unique performance in terms of spectral selectivity, tunability and high-frequency operation. Homogeneous MCFs allow both for highly unbalanced two-cavity OEOs as well as for multi-cavity vernier OEO operation where moderate and long cavity lengths (> 2 m) are compatible with a high-spectral purity and multi-GHz oscillation mode spectral separation. OEOs based on heterogeneous MCFs allow for ultralong cavity length (> 1 km) compatibility with high-spectral purity and multi-GHz oscillation mode spectral separation, while provide much lower phase noise operation. In addition, they bring the potential of featuring the tunability of the oscillation frequency by feeding the OEO system with a wavelength-tunable laser. The OEO structures proposed here still require further work on their optimization in terms of parameters and phase noise performance. This is the subject of on-going research and will be reported in due course.

Acknowledgments

The authors wish to acknowledge the financial support given by the Research Excellency Award Program GVA PROMETEO II/2013/012.